Eidgenössische Technische Hochschule Zürich
Swiss Federal Institute of Technology Zurich

eawag aquatic research

EIDGENÖSSISCHE TECHNISCHE HOCHSCHULE ZÜRICH
- ETH ZÜRICH

MASTER THESIS

Study of the relative importance of carbon and ethoxylated groups on the fate and transport of synthetic surfactants in natural soils

Author:
Marta M. Botella-Espeso

Supervisors:
Dr. Joaquín Jiménez-Martínez
Prof. Roman Stocker

A thesis submitted in the Chair of Groundwater and Hydrodynamics Institute of Environmental Engineering - IfU

September 2019

Eidgenössische Technische Hochschule Zürich
Swiss Federal Institute of Technology Zurich

Declaration of originality

The signed declaration of originality is a component of every semester paper, Bachelor's thesis, Master's thesis and any other degree paper undertaken during the course of studies, including the respective electronic versions.

Lecturers may also require a declaration of originality for other written papers compiled for their courses.

I hereby confirm that I am the sole author of the written work here enclosed and that I have compiled it in my own words. Parts excepted are corrections of form and content by the supervisor.

Title of work (in block letters):

RELATIVE IMPORTANCE OF CARBON AND ETHOXYLATED GROUPS ON THE FATE AND TRANSPORT OF SYNTHETIC SURFACTANTS IN NATURAL SOILS

Authored by (in block letters):

For papers written by groups the names of all authors are required.

Name(s):	**First name(s):**
BOTELLA ESPESO	MARTA MARÍA

With my signature I confirm that:

- I have committed none of the forms of plagiarism described in the 'Citation etiquette' information sheet.
- I have documented all methods, data and processes truthfully.
- I have not manipulated any data.
- I have mentioned all persons who were significant facilitators of the work.

I am aware that the work may be screened electronically for plagiarism.

Place, date

ZÜRICH, 05.09.2019

Signature(s)

For papers written by groups the names of all authors are required. Their signatures collectively guarantee the entire content of the written paper.

Eidgenössische Technische Hochschule Zürich - ETH Zürich

Abstract

Department of Civil, Environmental and Geomatic Engineering Institute of Environmental Engineering - IfU

Study of the relative importance of carbon and ethoxylated groups on the fate and transport of synthetic surfactants in natural soils

by Marta María Botella Espeso

This work studies the behavior of different non-ionic synthetic surfactant ethoxymers (alcohol polyethoxylates, AEOs) under unsaturated conditions from laboratory experiments performed in a flow cell. For this purpose, two different soils of a region irrigated with reclaimed water (Guadalete River basin, SW of Spain) were used. A first approximation of the water flow and transport of the selected ethoxymers using the HYDRUS-1D software package is presented. The model was calibrated using data collected in the experiments. Twelve different non-ionic surfactants with different carbon chains (C12, C14, C16, and C18) and ethoxylated groups (EO3, EO6, and EO8) were studied. Good agreement was achieved between the HYDRUS-1D simulations and experimental measurements for both, flow and reactive transport of all contaminants. For the adsorption process, most of the contaminants followed a Freundlich isotherm. However, as previously observed by other authors, a systematic comparison with Batch experiments revealed that the adsorption coefficient (K_d) was generally smaller underflow (field) conditions, whereas the exponent (β) did not show significant differences. The adsorption capacity of each contaminant was also analyzed as a function of clay content and soil organic matter, being higher as the longer the chains of ethoxylated groups were.

Acknowledgements

First of all, I would like to thank Dr. Joaquín Jiménez-Martínez, supervisor of this Master's Thesis, for his patience, constant feedback, and supervision during these last six months. This was a key factor for efficient work and obtaining the best results from this Master's Thesis project. As an industrial engineer, I am very happy to have been able to expand my knowledge and deepen in the exciting fields of groundwater and soil physics. I would also like to express my gratitude to Dr. Carmen Corada-Fernández (University of Cadiz, Spain), who has provided the experimental results.

I would also like to thank the group of fellow students and Ph.D. students that I had the chance of knowing at EAWAG and ETH, where I worked on my thesis project during the last few months. Being surrounded by such a motivated and professional group of colleagues was also important to get the best results from my work. I really appreciate their feedback and knowledge, always trying to help me get the best out of my work.

I would also like to thank my friends from ETH, IAESTE and MTEC, especially to Murod and Pepe, as well as my dearest Dodecahedron Improv group, for their constant support and company during these last few months of work. Always trying to bring up a smile from me whenever hard times were coming. All of them have been like my family, being abroad and far from home.

Finally, I want to thank my parents and my brother for constantly supporting my personal and academic targets, such as the challenge of finishing my master's degree in Zurich. The presentation of this Master's Thesis would never have been possible without your support.

List of figures

List of tables

Index

Chapter 1

Introduction

1.1 General framework

Groundwater contamination is often the result of human activities. This is a rising issue as the worldwide population density is increasing and the use of land is becoming more intensive. Pesticides applied to crops is one of the clearest examples regarding of groundwater contamination. In order to control and improve the quality of soils and aquifers, these compounds are now frequently monitored. (Hildebrandt, et al., 2008). There are, however, hundreds of other chemicals that are not considered in routine sampling campaigns and have the potential to threaten the sustainability of soils and groundwater resources.

Due to their wide array of applications, surfactants are among the most widely used synthetic chemicals in the world. They are not just used in the formulation of pesticides, but also paint products, pharmaceuticals, pulp, and paper industries, or PCPs (personal care products), among many others. Although their use is expanding to many other sectors, their main application is associated with the formulation of detergents, both for domestic and industrial use. Therefore, and as a consequence of their extensive use, in zones where treated wastewater is used for agricultural purposes, these emerging pollutants have been frequently found in the water bodies nearby (Topp, et al., 2012).

1. 1. 1 Surfactants

The term surfactant comes from surface-active agent. They are amphiphilic molecules, *i.e.*, with a hydrophobic and a hydrophilic part, which are being absorbed at the air-water interface. At this interface, surfactants align themselves in a way that the hydrophobic part is in the air and hydrophilic part is in the water. Consequently, surfactants decrease surface or interfacial tension. The hydrophobic tail is hydrocarbon, fluorocarbon or siloxane. Surfactants are typically classified based on their polar head as the hydrophobic tails are often similar. If the head group has no charge, the surfactant is called non-ionic. If the head group has a negative or positive charge, it is called anionic or cationic, respectively. If it contains both positive and negative groups, then the surfactant is called zwitterionic (Laurén, 2018).

Anionic and non-ionic surfactants are by far the most used ones in the industry. Anionic surfactants are mainly used in cleaning products like laundry detergents and shampoos. Non-ionic surfactants are often used as wetting agents and in the food industry. The rest, cationic and zwitterionic surfactants, are destined for special uses as they are more expensive to produce.

After use, residual surfactants and their degradation products, *i.e.*, metabolites, are released into the environment through urban and industrial wastewater by means of diffuse and punctual sources. In fact, surfactants and their metabolites constitute, undoubtedly, the organic contaminants reveling the highest concentrations in untreated wastewaters (Kolpin, et al., 2002). Despite the increasing volume of treated wastewater and the high removal efficiency in wastewater treatment plants, WWTPs (95-99%) (McAvoy, et al., 1998), the use of treated wastewater for irrigation and digested sewage sludge as fertilizer in agriculture is a common source of these pollutants. Flooding with water containing a considerable proportion of treated wastewater is one more example of how soils can be contaminated by surfactants (Oppel, et al., 2004). It is also worth noting that surfactants are also used for removing pollutants from the soil during remediation treatment processes (Lee, et al., 2000). Although the unsaturated zone (soil and vadose zone) acts as a buffer of these contaminants, when it reaches the limit of adsorption (surpassing its buffer capacity) and the existence of preferential flow (reducing the travel and residence time) makes them percolate and be incorporated into the hydrological cycle through the groundwater.

Between the large variety of surfactants, the most used are cleaning agents including alcohol ethoxylates (AEs), alkyl ethoxylate sulphates (AESs), and linear alkyl benzene sulfonates (LASs) (SRI Internacional, 1992). Elevated concentrations of these surfactants and their degradation products may affect organisms in the environment due to their estrogenic character (Guang-Guo, 2006) (Tubau, et al., 2010). Therefore, and due to their wide structural diversity, understanding the coupling of their natural abatement (by biodegradation and adsorption) and transport in soils is determinant for predicting their mobility and leaching to the groundwater. The polarity of the molecules and the structure and texture of the soil play a key role in delaying the transport of surfactants (Durán-Álvarez, et al., 2014). While LASs have been widely studied over the past decades in a variety of continental and marine systems, (González-Mazo, et al., 2004) (McAvoy, et al., 1993); (Takada & Ishiwatari, 1987) (Eichhorn, et al., 2002; Ding, et al., 1996), studies regarding the fate and transport of AEs and AESs have been very marginal.

1. 1. 2 Alcohol polyethoxylates (AEOs)

Alcohol polyethoxylates (AEOs) are a relevant group of non-ionic surfactants that are used commonly in domestic and commercial detergents, household cleaners and PCPs (Hermens & Droge, 2009). In WWTPs, AEOs are efficiently removed (up to 99%) by a combination of adsorption onto sludge and aerobic degradation (Szymanski, et al., 2003; Wind, et al., 2006), with total AEO concentrations in the effluents ranging from 0.92 to 22.7 μg/L in Europe and North America (Eadsforth, et al., 2006; Morrall, et al., 2006).

Significant quantities of these chemicals can reach aquatic ecosystems via direct discharges of different wastewaters. Once AEOs reach the aquatic environment, their behaviour is controlled by degradation and sorption processes. AEOs are found dissolved and associated with particulate material. Previous fieldwork showed that the amount of AEOs adsorbed on suspended solids can be up to 86% of the total measured concentration (Lara-Martín, et al., 2008). Partition coefficients have been measured ranging from 40 to 7000 L/kg (Cano & Dorn, 1996; Kiewiet, et al., 1996; Van Compernolle, et al., 2006), depending on the polarity and sorption capacity of different AEO homologs and/or ethoxymers. There are very few papers on AEOs sorption processes, and experiments were performed at very high concentrations (several ppm) (Podoll, et al., 1987). However, these chemicals are found in the environment in much lower concentrations, *e.g.*, in the water column are usually in the ppb range (Lara-Martín et al., 2011). Therefore, their behavior in terms of adsorption-desorption processes is not well characterized.

Although natural abatement of AEOs occurs in continental environments such as soils, delaying the arrival of these contaminants to the aquifer and minimizing the risk of groundwater pollution (Durán-Álvarez, et al., 2014), a number of them have been observed in aquifers in recent years. Laboratory experiments on the transport of these surfactants through unsaturated soils are not frequent, which are being generally assumed to behave like in fully saturated conditions (Henry & Smith, 2003). Yet, existing information on its performance in soils is very limited and specific studies are needed.

Over the last decade, AEOs sales have increased substantially as they have been used as a replacement of alkylphenol polyethoxylated (APEOs). Commercial AEOs are complex technical mixtures of homologs typically having from 12 to 18 carbon atoms in their hydrophobic alkyl chain bonded to a hydrophilic chain with a varying number of ethoxylate (EO) units (see Figure 1).

$$CH_3 -(CH_2)_{\varepsilon} -(O\text{-}CH_2\text{-}CH_2)_{\varepsilon'}\text{-}OH$$
$$11 \leq \varepsilon \leq 17$$
$$1 \leq \varepsilon' \leq 20$$

Figure 1. Molecular formula of AEOs.

1. 1. 3 Dependence on clay and organic matter

Experimental data for surfactant sorption in soils and sediments are quite abundant. Factors such as the length and nature of the surfactant polar chain and the nature of the solid surface must be taken into account (Lee, et al., 2011). It was shown that high clay mineral content in soils contributes significantly to the adsorption capacity of non-ionic surfactants (Yekeen, et al., 2019). However, the dependence of the adsorption processes on the organic matter has been assessed with disparate conclusions. Some results suggest a strong dependence of the adsorption capacity on organic matter, while others argue that they are weakly related (Lee, et al., 2011). Therefore, adsorption of non-ionic surfactants regularly shows a correlation with clays, while the high organic matter content soils produce divergent results (Yun-Hwei, 2000).

For the particular case of ethoxylated surfactants, two different adsorption mechanisms have been considered. The first one, involving linear adsorption, which depends directly on the alkyl chain length. This hydrophobic-based process explains why these chemicals are commonly found adsorbed into solid phases with high organic carbon content, such as solid suspensions, sediments or sewage sludge (Van Compernolle, et al., 2006). Nevertheless, other works show that AEOs do not seem to be affected by the organic carbon content in soils (Corada-Fernández, et al., 2015). The second mechanism tries to explain the observed non-linear sorption isotherms. It takes into account the hydrophilic interactions, via hydrogen bonds, between the ethylene groups and the clay fraction in sediments (Brownawell, et al., 1997; Cano & Dorn, 1996). In summary, sorption of AEOs is usually the result of the interaction of surfactant molecules combined with organic matter and clay (Droge & Hermens, 2007).

1. 1. 4 Scope and objectives

Surfactants in unsaturated conditions have often been assumed to behave like in fully saturated conditions. For the AEOs case, no systematic study depending on hydrocarbon chains and ethoxylated groups exist. Furthermore, no combined experimental and numerical analysis assessing flow and reactive transport processes for AEOs in unsaturated conditions has been carried out yet.

This thesis relies on previous fieldwork, with soil sampling in a region irrigated with reclaimed water and soils amended using sludge (Guadalete River basin, SW of Spain), and laboratory work, including isotherms determination and flow and transport experiments in a flow cell. This thesis pursues to improve the mechanistic understanding and prediction of the reactive transport of these surfactants in unsaturated soils. The goal is to analyse the behaviour of AEO surfactants and the relative importance of the hydrocarbon chain length and number of ethoxylated groups on the adsorption process as a function of organic matter and clay content in different soils. For that purpose, and to complete the exceptional laboratory work, I combine experimental results with numerical simulations, reproducing the flow and transport experiments. I demonstrate the need to recalculate the adsorption isotherm from the experimental conditions, due to the large differences observed concerning to the conventional Batch experiments. This aspect is key in assessing the risk of contamination in subsurface environments.

My research relies originally on previous experimental work performed for different samples of soil from Guadalete River Basin (SW Spain) which are often irrigated with reclaimed water from a nearby wastewater treatment plant and amended using sludge with the purpose of analyzing transport and reactive processes. In this thesis, I complement these laboratory experiments by presenting a numerical approach using simulations of the flow conditions imposed in the experiments.

I use HYDRUS-1D (Šimůnek, et al., 2006), a well-known computer model that simulates water, heat, and solute movement in variably saturated porous media. Firstly, I asses the flow of different transport experiments. A direct simulation of the flow is carried out, and once the hydrodynamic is well characterized, I solve the transport of AEOs using a non-equilibrium model. In this case, I use the inverse method to parametrize the transport model, minimizing the differences between measured and simulated concentrations.

A detailed description of the methods for both experiments and numerical simulations is presented in Chapter 2. Chapter 3 provides a general overview of the results obtained. A discussion is presented in Chapter 4, which establishes the comparison between the laboratory experiments and numerical simulations, as well as the dependence on clays and organic matter. Finally, conclusions and recommendations are summarized in Chapter 5.

Chapter 2

Materials and Methods

In this section, the methodology followed to perform the infiltration tests in a flow cell, simulate and determine the fate and transport of the target pollutants in two different soils is described. Soil samples were taken is a region where agricultural soils are irrigated with reclaimed water and amended using sludge (Guadalete River basin, SW of Spain). A large volume of wastewater from the cities and towns is treated and discharged into the river. The soil samples were taken from two different locations, locally called Rio Viejo (soil core 1) and Guadalcacín (soil core 2).

2.1 Soil samples characterization

Different techniques and standards were used to determine soil physical properties (Table 1). Grain size distribution was determined according to ASTM D 422-63 and Gee and Or (2002). Soil textural class was defined according to the USDA system. Bulk density was determined following the method proposed by Grossman and Reinsch (2002). Saturated hydraulic conductivity was empirically determined in the laboratory (Reynolds & Elrick, 2002) since this hydraulic property is highly affected by the concentration of surfactants in the solution. Chemical properties were determined from disturbed samples. Organic carbon (OC) content was determined by dichromate oxidation, using the method proposed by Gaudette et al. (1974), with the El Rayis (1985) modification (Table 1).

2.2 Infiltration experiments

The infiltration tests were performed in an intermediate scale flow cell (49.5 x 58.7 x 1 cm, see Figure 2). Each flow cell was filled with the different soils keeping horizons order and thickness as *in-situ*. They were repacked trying to replicate the original bulk density (Table 1). The base of the flow cell was completed with silica sand (Ottawa sand) to ensure drainage. Some studies recommend long experimental times for mixtures of AEOs (Kiewiet, et al., 1996; Brownawell, et al., 1997), as exchanges between different homologs or ethoxymers can occur before reaching steady-state. However, using shorter times has also been suggested (Brownawell, et al., 1997; Cano & Dorn, 1996) to avoid the biological degradation of these non-ionic surfactants. Results obtained from control solutions of AEOs demonstrated that biodegradation is negligible during sorption experiments (Travero-Soto, et al., 2014). Therefore, we decided to perform long infiltration experiments, having 192 hours for the soil core 1, and 69 hours for soil core 2. Soil samples were collected at the same depths before and after the experiments in order to characterize the mobility of the targeted compounds. Data included water content and total concentrations (adsorbed + dissolved) of the contaminants at each selected depth.

An AEOs solution was applied during the total duration of the experiments at a constant flow rate using a peristaltic pump and a drip irrigation system. For soil cores 1 and 2 were used 0.083 and 0.43 cm^3/h, respectively. Noteworthy is that the solution was being permanently homogenized by a magnetic stirrer in order to avoid the accumulation of these compounds at the air-water interface. The solution applied was a mixture of different polyethoxylated alcohols (AEOs). The test was carried out at a constant temperature so that the impact on the soil hydraulic properties could be minimized.

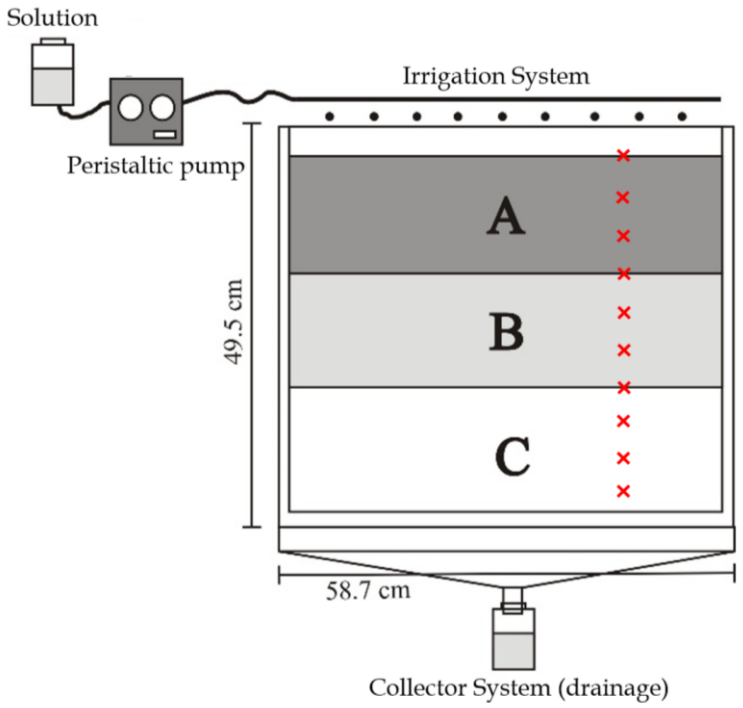

Figure 2.Flow cell and dimensions. Drip irrigation and collector system for drainage. Sketch for soil core 1, soil horizons and selected sample points (crosses).

Table 1. Physico-chemical and hydraulic properties of soil samples. OC is the soil organic carbon content, ρ_b is the bulk density, θ_r, and θ_s are the residual and saturated water content, respectively, α the inverse of the air entry value, n pore size distribution index, and K_s is the saturated hydraulic conductivity.

Horizon	Depth	Texture [%]			OC [%]	ρ_b	Soil type	θ_r	θ_s	a	n	K_s
	[cm]	Sand	Silt	Clay		[g/cm³]		[cm³/cm³]	[cm³/cm³]	[1/cm¹]	[-]	[cm/h]
1A	0-19	41.71	54.68	3.61	1.1	1.3349	Silty Loam	0.0343	0.3638	0.0091	1.5477	2.67
1B	19-30.5	84.42	14.58	1	0.3	1.5154	Loamy Sand	0.0392	0.3739	0.0436	2.1783	8.97
1C	30.5-47.1	100	0	0	0	1.9438	Sand	0.049	0.2663	0.0295	4.036	26.23
2A	0-14	64.36	33.29	2.35	1.2	1.6499	Sandy Loam	0.0277	0.3639	0.0507	1.3946	1.50
2B	14-18.5	46.4	51.88	1.72	0.6	1.6868	Silt Loam	0.0252	0.427	0.0319	1.3423	0.95
2C	18.5-29.5	41.17	54.77	4.06	0.6	1.7095	Silt Loam	0.0277	0.3557	0.0245	1.3515	0.66
2D	29.5-46.5	100	0	0	0	2.0098	Sand	0.0492	0.2563	0.0288	4.1103	23.62

2.3 Chemicals and adsorption isotherms

The solution used in the experiments was a mixture of homologues (C12, C14, C16, and C18) of polyethoxylated alcohols (AEOs). Three pure ethoxymers (3, 6 and 8 EO ethoxylated groups) per homologue were used (see Figure 1), all of which were in the same proportion in the solution. The different ethoxymers of AEOs were analysed according to the methodology proposed by Lara-Martín, et al (2006).

Adsorption isotherms were determined by conventional Batch experiments. The soil was stirred with water and the set of contaminants (using different concentrations of 5, 10, 25, 50, 100, and 200 ng/cm^3) for 24 h. Data could be fitted by a Freundlich model for all surfactants used, in agreement with previous studies (Brownawell, et al., 1997; John, et al., 2000; John, et al., 2009).

2.4 Non – equilibrium chemical transport

For the simulation of the water flow and reactive transport of the selected ethoxymers, the HYDRUS-1D code was used (Šimůnek, et al., 2006). The program may be used to analyse water and solute transport in variably saturated porous media. Flow and transport equations described below are solved numerically using standard Galerkin-type linear finite element schemes subjected to appropriate initial and boundary conditions (Šimůnek, et al., 2015).

2. 4. 1 Unsaturated flow

The unsaturated flow is solved assuming the gas phase does not play an important role in the liquid phase displacement. For uniform one-dimensional flow in a partially saturated porous medium the equation governing the flow is given by the modified Richards equation expression:

$$\frac{\partial \theta}{\partial t} = \frac{\partial}{\partial x}\left[K\left(\frac{\partial h}{\partial x} + 1\right)\right] - S \tag{1}$$

where θ is the volumetric water content [L^3 L^{-3}], h the soil pressure head [L], S the sink term [T^{-1}], x the spatial coordinate in the vertical direction [L], t time [T]. K is the unsaturated hydraulic conductivity [L T^{-1}], and as follow:

$$K(h, z) = K_s(x) K_r(h, x) \tag{2}$$

where K_r is the relative hydraulic conductivity and K_s the saturated hydraulic conductivity [L T^{-1}].

Water retention and unsaturated hydraulic conductivity function for each soil layer were obtained by the van Genuchten-Mualen expression (Mualem, 1976; van Genuchten, 1980):

$$\theta(\mathrm{h}) = \begin{cases} \theta_\mathrm{r} + \dfrac{\theta_\mathrm{s} - \theta_\mathrm{r}}{[1 + |\alpha \mathrm{h}|^\mathrm{n}]^{1-1/\mathrm{n}}} & \mathrm{h} < 0 \\ \theta_\mathrm{s} & \mathrm{h} \geq 0 \end{cases} \tag{3}$$

$$K(h) = K_s S_e^l \left\{1 - \left[1 - S_e^{n/(n-1)}\right]^{1-1/n}\right\}^2 \quad (4)$$

where S_e is the effective saturation:

$$S_e = \frac{\theta(h) - \theta_r}{\theta_s - \theta_r} \quad (5)$$

and $\theta(h)$ the volumetric water content at pressure head h or water retention function. The parameters θ_r and θ_s are the residual and saturated water content, respectively, α the inverse of the air entry value, n pore size distribution index. In order to reduce the number of parameters, l is commonly assumed to be 0.5 (Mualem, 1976). These parameters were estimated using ROSETTA (Schaap, et al., 2001), a pedotransfer function model that predicts hydraulic parameters from soil texture and related data, *e.g.*, soil bulk density (Table 1).

2. 4. 2 Reactive transport

The transport equation, beyond the advection-dispersion processes, it includes degradation and adsorption as reactive processes:

$$\frac{\partial \theta C_w}{\partial t} + \frac{\partial \rho_b C_s}{\partial t} = \frac{\partial}{\partial x}\left(\theta D \frac{\partial C_w}{\partial x}\right) - \frac{\partial q C_w}{\partial x} - \mu \theta C_w \quad (6)$$

where C is the chemical concentration [M L^{-3}], and w and s the subscripts for the concentration in the interstitial water and adsorbed in the solids, respectively; q is the water flux [LT^{-1}]; μ is the degradation constant for the chemical in liquid phase [T^{-1}]; ρ_b is the bulk density of the soil [M L^{-3}]. D is the dispersion coefficient [L^2 T^{-1}] according to (Bear, 1972):

$$\theta D = \lambda |q| + \theta D_m \tau_w \quad (7)$$

where D_m is the molecular diffusion coefficient [L^2 T^{-1}]; λ the longitudinal dispersivity [L]. The tortuosity τ_w has been computed according to (Millington & Quirk, 1961) as:

$$\tau_w = \frac{\theta^{7/3}}{\theta_s^2} \quad (8)$$

2. 4. 3 Sorption process

The isotherms of adsorption that relates C_s and C_w is defined as:

$$C_s = \frac{K_d C_w^\beta}{1 + \eta C_w^\beta} \quad (9)$$

where K_d [L^3M^{-1}], β [-] and η [L^3M^{-1}] are the coefficients of the isotherm. The isotherms of Freundlich, Langmuir and lineal are specific cases of the defined one. When $\beta = 1$, the isotherm is Langmuir, if $\eta = 0$ the isotherm is Freundlich, while if both $\beta = 1$ and $\eta = 0$ then it would be a lineal isotherm (Figure 3).

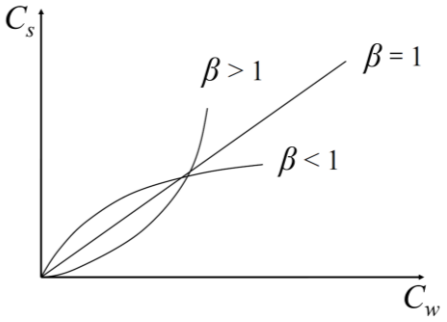

Figure 3. The isotherms of adsorption that relates C_s and C_w. When $\beta = 1$, the isotherm is lineal, while if both $\beta < 1$ and $\beta > 1$ the isotherm is Freundlich. Langmuir isotherm has not been plotted.

2. 4. 4 Scaling of the hydraulic properties

Analogously as for the temperature, the effect of changes in concentration on surface tension and viscosity, and consequently on water retention (pressure-water saturation) and hydraulic conductivity functions, were incorporated from the Smith and Gillham (1994; 1999) scale relationships. From the capillary pressure-surface tension ratio, the effect of a solution on the pressure-saturation ratio can be predicted from the relationship between the surface tension of pore water as a function of concentration (σ) and the surface tension for pure water (σ_o):

$$h(\theta, C_w) = \frac{\sigma}{\sigma_o}\, h(\theta, C_{wo}) \tag{10}$$

where $h(\theta,C_{wo})$ the pressure for water content and a reference concentration C_{wo} (C_{wo} is 0 for pure water), and $h(\theta,C_w)$ the soil pressure head scaled to the same water content and concentration c.

The hydraulic conductivity as a function of concentration $K(\theta,C_w)$ is computed from the relation between viscosity of the solution and pure water:

$$K(\theta, C_w) = \frac{v}{v_o}\, K(\theta, C_{wo}) \tag{11}$$

here $K(\theta,C_w)$ is the concentration-dependent unsaturated hydraulic conductivity obtained from the hydraulic conductivity for pure water and the same water content $K(\theta,C_{wo})$ and according to the relative viscosity v/v_o.

2.5 Model implementation and inverse method

A direct simulation was used to solve flow in both infiltration experiments. The inverse solution was only needed to be used in the case of θ_s of the soil core 2 where a higher flow was applied. Conservative solute transport (tracer test) was performing adopting representative dispersivity values from the literature. The inverse solution was carried out to solve the transport of the contaminants in order to parametrize the reactive processes according, and in particular the adsorption process, to the actual experimental conditions.

2. 5. 1 Spatial discretization, initial and boundary conditions

A finite element mesh was created using the graphical process-editor available in HYDRUS-1D. The grid was discretized with 90 equidistant nodes separated by 0.5 cm. Three and four different layers were settled for soil core 1 and 2, respectively, while the mass balance was defined for the whole system.

One value per soil horizon was considered as initial water content and concentration of the 12 ethoxymers analysed during the experiment. No hysteresis in the water retention functions was considered and as boundary conditions for the water flow, constant flow condition (q, 0.083 and 0.43 mL/min, for soil core 1 and 2, respectively) at the surface and free drainage at the bottom were considered. No evaporation was considered at the upper limit. For transport, variable concentration and free drainage were adopted for the upper and lower limit, respectively.

2. 5. 2 Surfactants: diffusion and degradation

The same molecular diffusion coefficient D_m=1.008 10^{-2} cm^2/h (Song, et al., 2006) was used for all contaminants, and a degradation constant μ (1/h) for each of them (Human and Environmental Risk Assessment on ingredients of European household cleaning products, AEOs) (Table 2). The first order-rate coefficient for one site or two sites non-equilibrium adsorption, *i.e.*, mass transfer coefficient for solute exchange between mobile and immobile liquid regions, was estimated obtaining an average value of k = 6.5 1/h. From the laboratory tests, it has also been concluded that the kinetic of all surfactants used is of the same order of magnitude, therefore, using the same value for all of them.

Table 2. Degradation constant of the different AEOs surfactants used in the experiments by hydrocarbon chains and ethoxylated groups.

Hydrocarbon chain	**EO group**	μ
		[1/h]
C12	EO3	0.1733
	EO6	0.0866
	EO8	0.0578
C14	EO3	0.1733
	EO6	0.0866
	EO8	0.0866
C16	EO3	0.1733
	EO6	0.0866
	EO8	0.0866
C18	EO3	0.0866
	EO6	0.1733
	EO8	0.1733

2. 5. 3 Surfactant concentration impact on surface tension

The primary impact of surfactants on unsaturated flow is through the dependence of soil water pressure on surface tension. This dependency can be expressed by Bear (1972):

$$h = -\frac{2\sigma \cos\gamma}{\rho g r} \tag{12}$$

where h is soil water pressure head or capillary pressure, σ is surface tension, ρ is the solution density, g is the gravitational acceleration, γ is the contact angle, and r is the radius of an equivalent circular tube. Because soil water content is a function of soil water pressure, solutes that decrease the surface tension at the soil-air interface, also directly affect water retention in unsaturated porous media (Salezadeh & Demond, 1994; Smith & Gillham, 1994; 1999; Lord, et al., 1997; 2000).

In addition to the impact of surfactants on the soil water retention relationship, surfactant concentration gradients can cause capillary pressure gradients in unsaturated porous media. At a given soil water content (and thus a fixed radius of curvature in equation 12) the soil water pressure head in an unsaturated porous medium wetted with a surfactant solution will be higher (less negative) than if the porous medium was wetted with pure water. Because of this, there will be a tendency for unsaturated flow to occur from contaminated regions (higher pressure, lower surface tension) toward cleaner regions (lower pressure, higher surface tension).

The influence of surfactant structures on the equilibrium surface properties, and adsorption behaviors at the air-water interface have been investigated systematically (Paweena, et al., 2017). At very low concentrations, AEOs groups are maintained at the same surface tension equilibrium level. For the range of surfactant concentrations used in these experiments (1 10^{-7} and 2.6 10^{-7} µmol/L; 1 10^{-10} and 2.6 10^{-9} µmol/cm^3, respectively), the impact on surface tension stays close to zero. Consequently, no changes in the hydraulic properties were considered.

2. 5. 4 Conservative transport

Dispersivity (λ) in the one-dimensional convection-dispersion equation (7) is known to be a sensitive parameter for predicting the mass that leaches through the vadose zone to the groundwater. A large database of dispersivities, among many other parameters, was provided by (Vanderborght & Vereecken, 2007) from intensive studies in soils. Dispersivity was found to increase with increasing transport distance and scale of the experiment, and larger dispersivities were observed for saturated than for unsaturated flow conditions. No significant effect of soil texture on dispersivity was observed, but the interactive effects of soil texture and flow rate on dispersivity were significant.

Dispersivity is hard to estimate (Perfect, et al., 2002) and no specific methods to measure it were carried out during the experiment. Therefore, intensive bibliography research was carried out to delimit this parameter for each soil horizon (Table 3).

Table 3. Dispersivity of the different soil horizons.

Horizon	λ
	[cm]
1A	0.6
1B	1.87
1C	1.3
2A	2.37
2B	3.04
2C	3.04
2D	1.3

2. 5. 5 Reaction versus transport processes

The transport regime is characterized by two dimensionless numbers. The Péclet number, which compares the relative importance of advective (τ_a) and diffusive (τ_d) effects during transport. Here, computing it as $Pe = \tau_d/\tau_a = (u/D_m)\Delta x$ (El-Kadi & Ge, 1993), where u is the mean water velocity ($u = q/\theta$), and Δx the spatial discretization, 0.5 cm in this case. The relative importance of transport to chemical reactions is measured by the Damköhler number (Da), representing the ratio of advection (τ_a) to reaction (τ_r) time scales, $Da = \tau_a/\tau_r$. The reaction time scale is defined by the kinetics of adsorption (k) in well-mixed conditions $\tau_r = 1/(C_{wo}k)$ (Connors, 1990). Chemical reactions can thus be classified as mixing-driven (or mixing-limited), when the reaction is fast compared to advection ($Da>>1$), or kinetics-driven ($Da<<1$). The average Pe and Da were smaller than 1. Based on these two criteria, we assumed an equilibrium or quasi-equilibrium model, *i.e.*, the adsorption process can be considered a fast irreversible reaction.

Chapter 3

Results

This chapter compiles the most relevant results from the performed numerical analysis. It includes the flow and reactive transport modelling for the targeted contaminants. First, the modelling results have been compared with the measured soil water content and concentration at different depths from laboratory experiments, in order to evaluate the model reliability and accuracy. Second, adsorption isotherms parameterized from the numerical simulations have been compared to those obtained from Batch experiments. In this section, we also assess the impact of the clay and organic matter content on the abatement of these contaminants in the liquid phase.

3. 1 Flow and reactive transport modelling

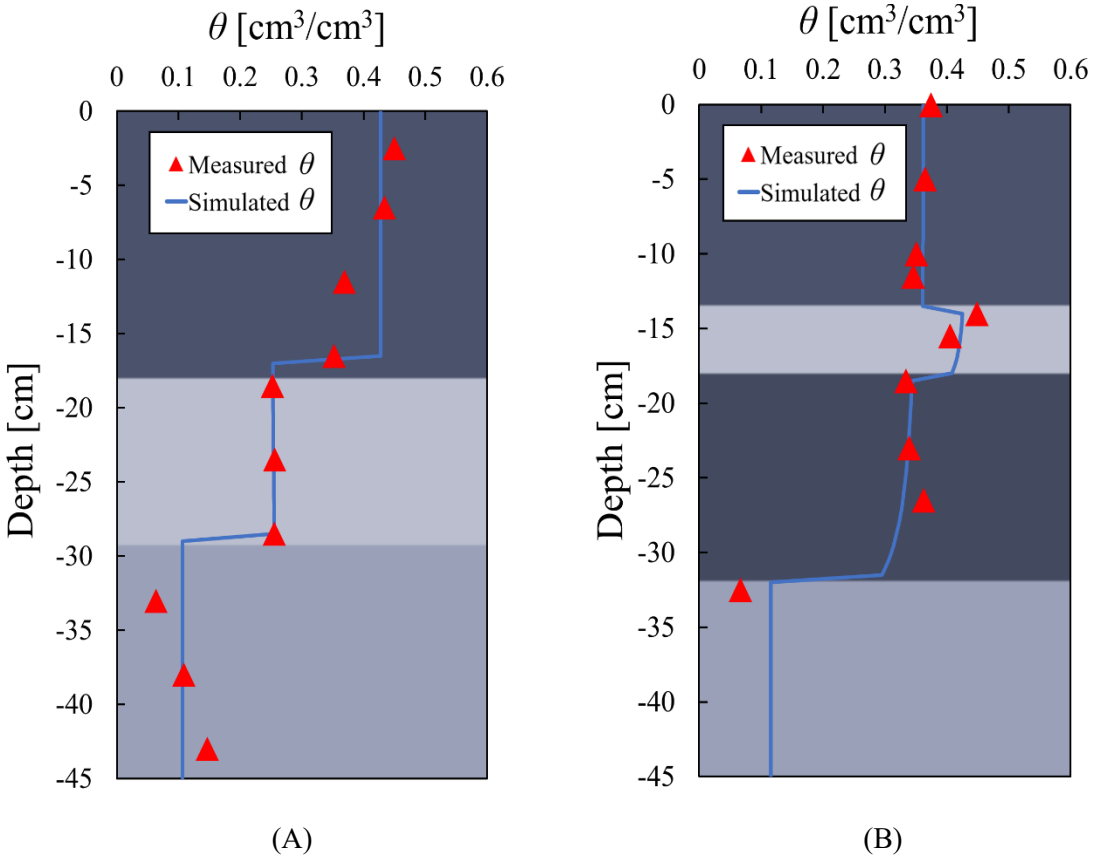

Figure 4. Measured (triangles) and simulated (solid line) soil water content θ [cm^3/cm^3] at different depths. (A) Soil core 1, R^2 = 0.93. (B) Soil core 2, R^2 = 0.97. 192 and 69 hours respectively, after starting the experiment.

Water content profiles for both studied soils are presented in Figure 4. The plots show water content changes through the different soil cores and between the different soil horizons. Two transitions between horizons in soil core 1 (three horizons) and three in soil core 2 (four horizons) can be easily identified. The high coefficient of determination R^2 (>0.9) between numerical and experimental results in both soil cores indicates the reliability of the direct simulation in reproducing the hydrodynamics in the system.

Once hydrodynamic was well characterized, reactive transport models were performed for the twelve different AEOs (Table 2) and in each flow cell. Figure 6.B shows a final total concentration ($C_s + C_w$) profile for C14AEOEO8. A total of 24 profiles, 12 per flow cell, were obtained in this analysis. Similarly to the flow model, experimental concentrations were compared with simulation results at different depth. This allowed to parametrized the isotherm of adsorption (β and K_d, eq. 9) for each surfactant in each soil horizon.

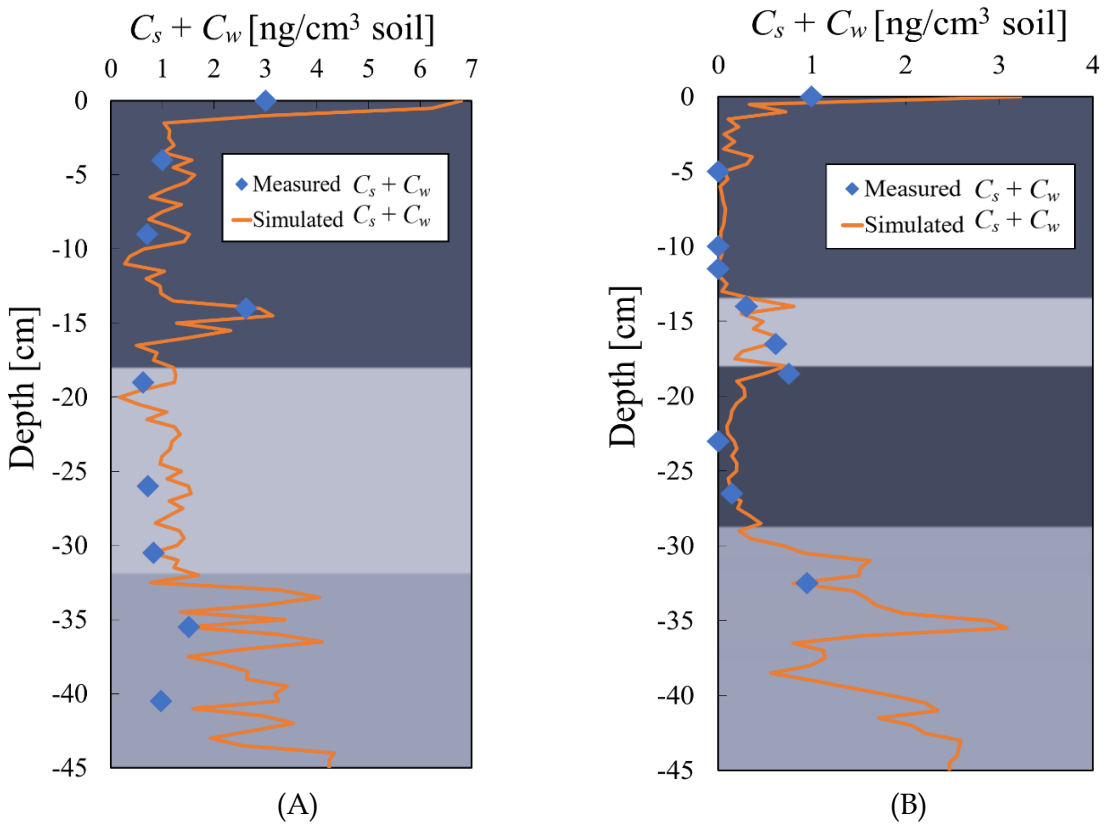

Figure 5. Measured (rhomboids) and simulated (solid line) total concentration ($C_s + C_w$) [ng/cm^3 of soil] for C14AEOEO8 at different depths. (A) Soil core 1, R^2 = 0.650. (B) Soil core 2, R^2 = 0.613. 192 and 69 hours respectively, after starting the experiment.

Figure 6 compares measured versus simulated data, for water content and AEOs concentration at the same depths. The results obtained for soil water content display a clear 1:1 drift with an R^2 = 0.94 (Figure 6.A). However, a larger scattering is observed for total surfactant concentrations (Figure 6.B), remaining the 83% of the values around the 1:1 line between 0 and 4 ng/cm^3 of soil.

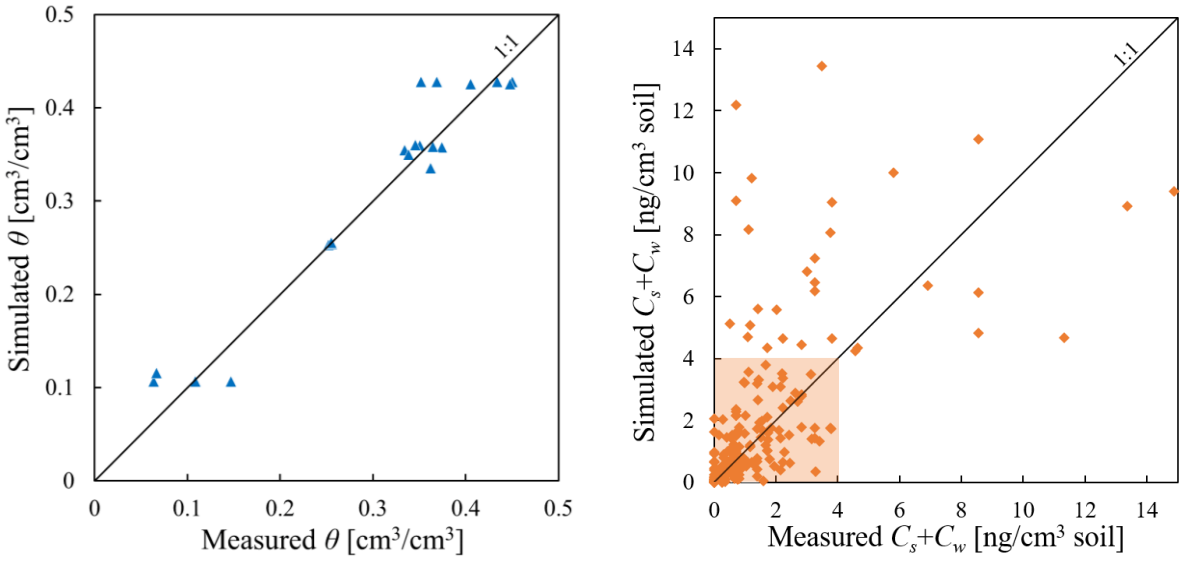

(A) (B)

Figure 6. (A) Simulated vs. measured soil water content, θ [cm^3/cm^3]. (B) Simulated vs. measured total concentration, (C_s+C_w) [ng/cm^3 of soil] for all targeted surfactants. Marked area for concentrations < 4 ng/cm^3 of soil (84% of the data points).

3. 2 Adsorption isotherms: measured vs. simulated

Freundlich isotherm parameters (K_d and β) for each surfactant and soil horizon are computed. Differences between surfactants and between simulated and experimentally obtained K_d and β are shown in Figure 7. Results are presented by carbon chain length (C12, C14, C16, and C18) and number of ethoxylated groups (EO3, EO6, and EO8).

Figure 7.A shows K_d (expressed for simplicity as $\log_{10} K_d$) the measured values for C12, C14 and C18 ranging from 1.62 10^{-7} to 1.96 10^{-5} (cm^3/ng), while values belonging to C16 are narrowed from 8.51 10^{-7} to 3.8 10^{-6} (cm^3/ng). On the contrary, all values obtained from the simulations are in the same narrow range, with values ranging from 3.72 10^{-8} to 4 10^{-7} (cm^3/ng). Results obtained as a function of the ethoxylated groups are shown in Figure 7.B. EO3 shows a narrower range than EO6 and EO8, between 7.47 10^{-7} and 5.89 10^{-6} (cm^3/ng) for measured values, but very similar for the simulated ones as for carbon chain length. In general, simulated K_d was between 1 and 2 orders of magnitude smaller than measured one from Batch experiments.

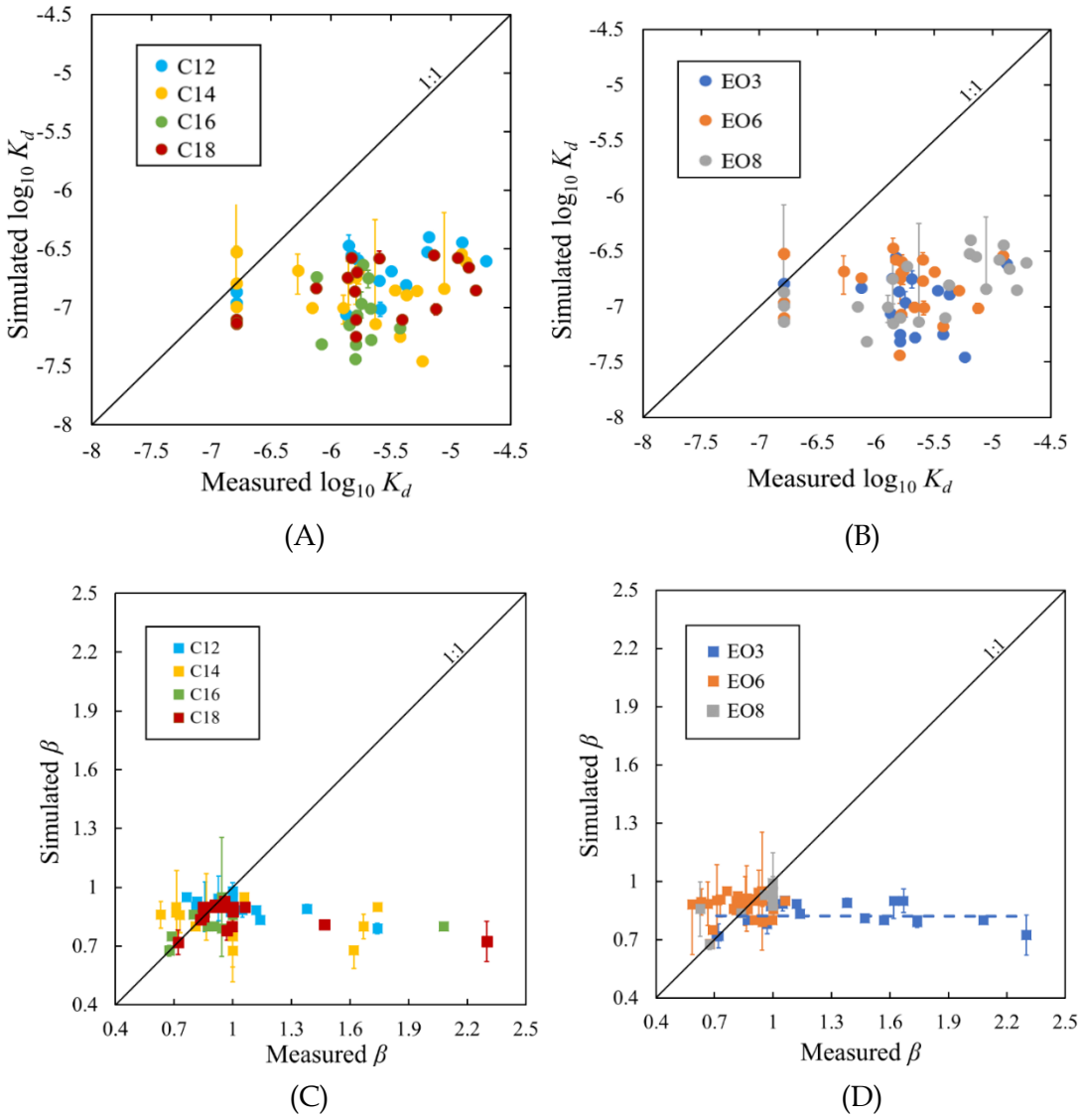

Figure 7. (A) Simulated vs. measured $\log_{10} K_d$ [cm^3/ng] plotted by carbon chains: C12 (blue), C14 (yellow), C16 (green) and C18 (red). (B) Simulated vs. measured $\log_{10} K_d$ [cm^3/ng] plotted by ethoxylated groups: EO3 (blue), EO6 (orange) and EO8 (grey). (C) Simulated vs. measured β plotted by carbon chain: C12 (blue), C14 (yellow), C16 (green) and C18 (red). (D) Simulated vs. measured β plotted by ethoxylated group: EO3 (blue), EO6 (orange) and EO8 (grey). Bars indicate 95% confidence intervals for the calibrated parameters.

A similar analysis was performed to evaluate the behavior of the β parameter (Figure 7.C and .D). Measured values as a function of the carbon chain range from 0.6 to 2. While those corresponding to the simulations range from 0.6 to 0.95 (Figure 7.C). Although some of them deviate from the line 1:1, similar β values were obtained from simulations and experiments. However, the plot by ethoxylated groups (Figure 7.D) reveals a trend in β for the measured EO3 group.

Error bars in Figure 7 refer to the errors obtained in HYDRUS for each parameter by inverse solution (simulated results, y-axes). Errors for the measured values (x-axes) are not plotted due to the difficulties found to compute them properly (*i.e.*, not taken into account during the experimental determinations). Nevertheless, the experimental errors, including manipulator and instrumental errors, are known for incorporating a high degree of uncertainty.

3. 3 K_d dependence on clay and organic matter

Figure 8 depicts the clay content dependence on average K_d. Similar trends by carbon chain length are observed for both simulated and measured K_d (Figure 8.A). For those values corresponding to the measured ones, a stable K_d around 2 10^{-6} (cm^3/ng) from 2% of clay content is observed independently of carbon chain length. By ethoxylated group Figure 8.B, the stable K_d value is around to 4 10^{-6} (cm^3/ng). Similar trends, although of less magnitude, are observed for simulated K_d as a function of clay content for both by carbon chain length and by number of ethoxylated group.

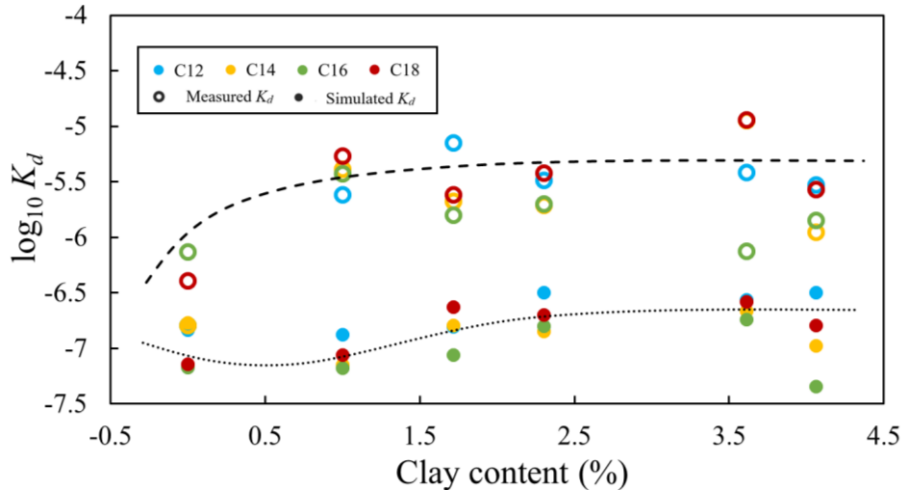

(A)

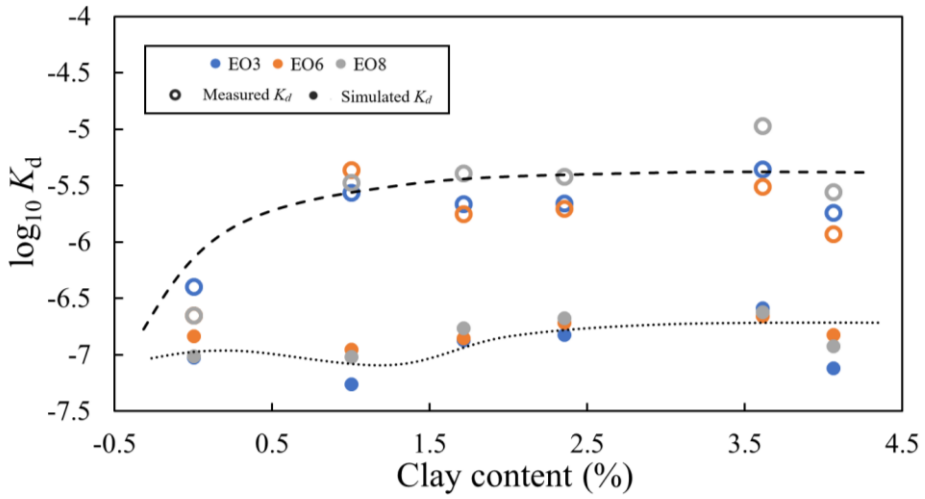

(B)

Figure 8. (A) Average measured (empty circles) and simulated (filled circles) K_d values as a function of clay content, plotted by carbon chains: C12 (blue), C14 (yellow), C16 (green) and C18 (red). (B) Average (empty circles) and simulated (filled circles) K_d values as a function of clay content, plotted by ethoxylated groups: EO3 (blue), EO6 (orange) and EO8 (grey).

Average K_d values as a function of the organic matter content are plotted Figure 9. Measured K_d reaches an asymptotic value of 3.16 10^{-6} and 5.3 10^{-6} (cm^3/ng) for OC > 0.3% in both classifications, by carbon chain length (Figure 9.A) and ethoxylated group (Figure 9.B), respectively. Average simulated K_d presents similar trends in both classifications as for clay content.

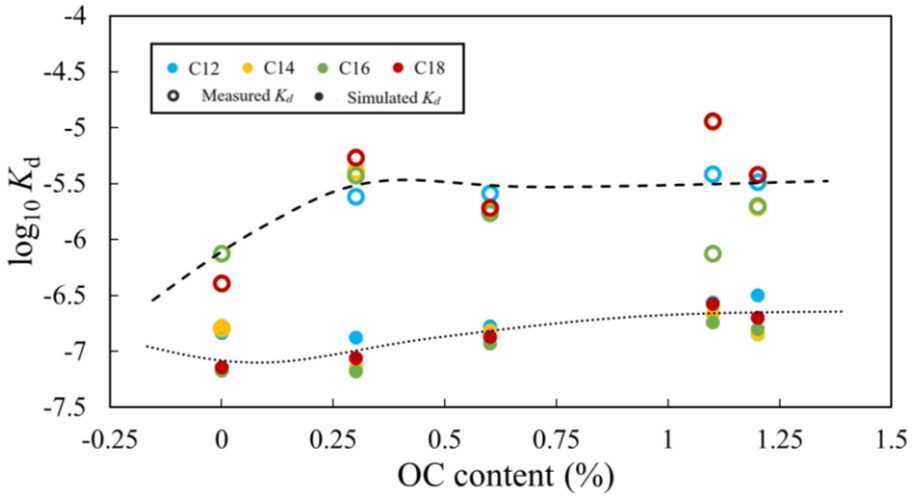

(A)

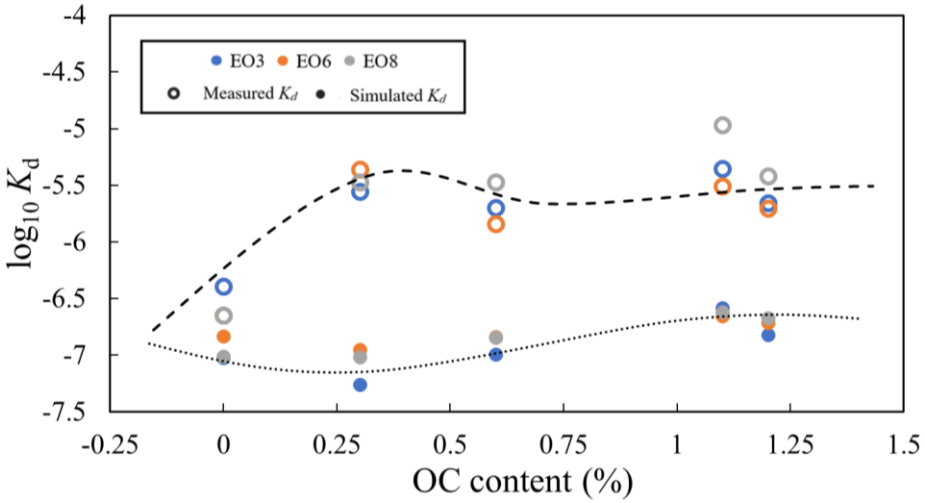

(B)

Figure 9. (A) Average measured (empty circles) and simulated (filled circles) K_d values as a function of organic matter content, plotted by carbon chains: C12 (blue), C14 (yellow), C16 (green) and C18 (red). (B) (A) Average measured (empty circles) and simulated (filled circles) K_d values as a function of organic matter content, plotted by ethoxylated groups: EO3 (blue), EO6 (orange) and EO8 (grey).

3. 4 β dependence on clay and organic matter

The dependence of the β parameter of the Freundlich isotherm on clay content and organic matter are shown hereunder. β shows a similar trend as a function of clay (Figure 10) and organic matter (Figure 11) content. However, important differences are observed between measured and simulated values. While for measured β show an important variability as a function of clay and organic matter content, with no apparent trend, simulated β is pretty stable independently of the clay and organic matter content.

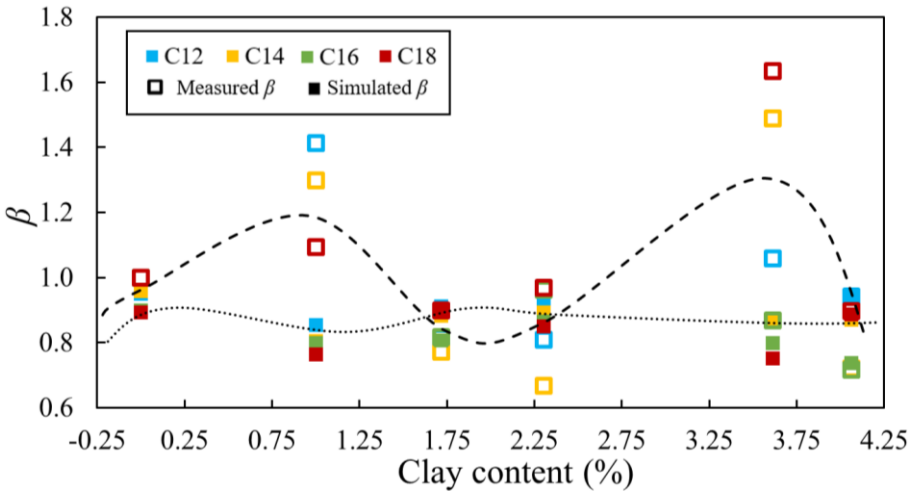

(A)

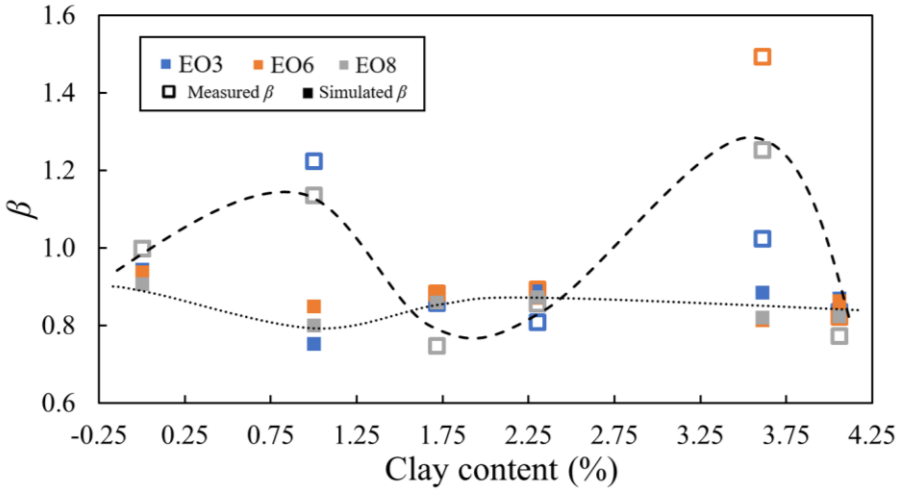

(B)

Figure 10. (A) Average measured (empty circles) and simulated (filled circles) β values as a function of clay content, plotted by carbon chains: C12 (blue), C14 (yellow), C16 (green) and C18 (red) and the trend lines. (B) Average measured (empty circles) and simulated (filled circles) β values as a function of clay content, plotted by ethoxylated groups: EO3 (blue), EO6 (orange) and EO8 (grey) and the trend lines.

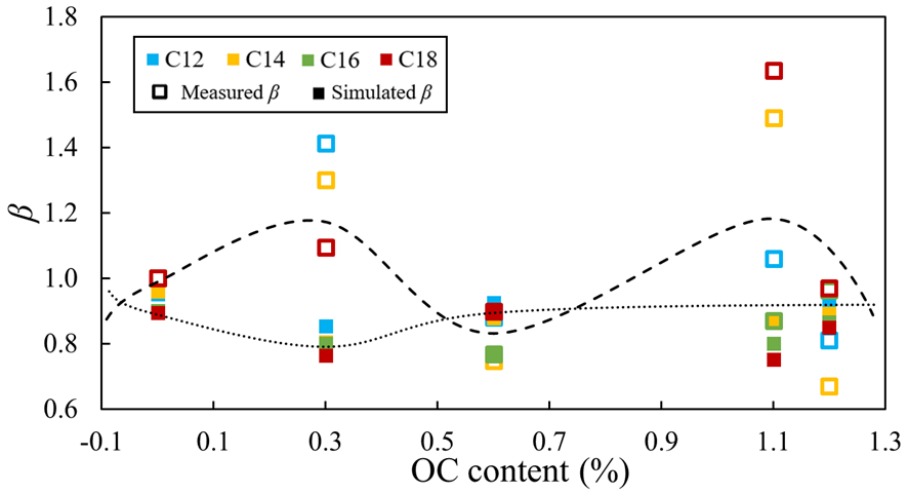

(A)

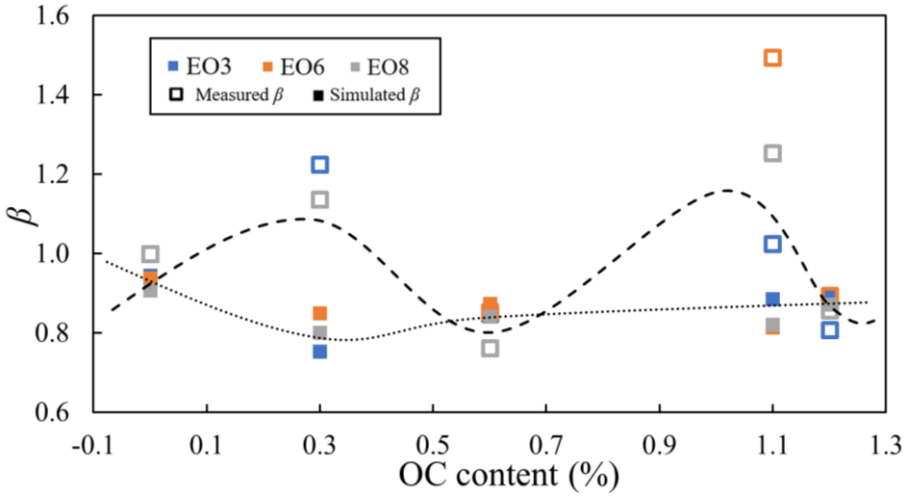

(B)

Figure 11. (A) Average measured (empty circles) and simulated (filled circles) β values as a function of organic matter content, plotted by carbon chains: C12 (blue), C14 (yellow), C16 (green) and C18 (red) and the trend lines. (B) Average measured (empty circles) and simulated (filled circles) β values as a function of organic matter content, plotted by ethoxylated groups: EO3 (blue), EO6 (orange) and EO8 (grey) and the trend lines.

Chapter 4

Discussion

4. 1 Goodness of the model

The direct flow model, *i.e.*, using soil characterization data and ROSETTA estimations, carried out for both experimental cells captured well the hydrodynamics in the system. Soil horizons, with different texture and hydraulic parameters, induced changes in water content and water velocity along with the profile. Soil horizons can be easily identified from the water content profile (Figure 4). The performance of the flow model was evaluated both in terms of goodness of fit to available water content measurements and plausibility of the model parameters. Figure 6.A shows a scatter plot of the measured and calculated soil water content. The absence of scattering between measured and simulated soil water content and an $R^2 > 0.9$ in both experimental cells indicate the appropriateness of the flow parameterization. In other words, this indicates the reliability of the laboratory and ROSETTA estimations, and therefore, the robustness of the flow model.

Although dispersity values were taken from the literature (and based on a large database), a sensitivity analysis for it demonstrates the low impact on the conservative and reactive transport results. Due to the horizon thicknesses and the numerical spatial discretization adopted, ranges of dispersivity used were smaller than one order of magnitude.

The reactive transport model was based on the flow and conservative transport parameterization. In this case, the inverse method was used to characterize the adsorption process for each surfactant underflow experimental conditions. Note that the impact of surfactants on the hydraulic properties was discarded, and the kinetics of adsorption and disintegration were well known. Similarly to the water flow model, the performance of the calibrated model is evaluated both in terms of goodness of fit to available total concentration (adsorbed + dissolved) measurements and plausibility of the model parameters. Although R^2 obtained for each surfactant was not as good as for soil water content, the reactive transport model captured quite well the shape of the total concentration profiles (Figure 5). Note that differences between measured and simulated total concentrations were expected due to the uncertainty associated with the laboratory determination of very low concentrations (ng/cm^3), even using the most advanced measurement tool and protocols. The scatter plot of the measured versus simulated total concentration shows an important scattering, *i.e.*, deviation from the line 1:1, especially for total concentrations above 4 ng/cm^3 (Figure 6.B). Points located further from the line 1:1 are those corresponding to the first sampling point at 0 cm depth. These points are located right at the interface between the applied water and the soil surface, generally presenting a high total concentration value and having an added difficulty in a reliable determination both experimentally and numerically. Discriminating these points, the model performance increases considerably. Nevertheless, the fitted parameter K_d for each surfactant was around 1.5 order of magnitude smaller than the ones obtained from Batch tests, as indicated by the literature for these compounds and underflow conditions.

4. 2 Adsorption under flow conditions

Several studies have exposed that adsorption coefficients obtained through Batch experiments are usually higher than those observed in the field. Such studies emphasize that the K_d value of Ni, Mn, and Cr in Batch tests is higher than one order of magnitude than in common natural soils (Rodriguez & Candela, 2005). But this fact does not only seem to be fulfilled for the adsorption of metals. Regarding surfactants, results obtained in (Travero-Soto, et al., 2014) also reveal lower orders of magnitude for adsorption coefficients in the field.

Figure 7.A and .B confirm the described behavior. K_d values in the Freundlich model were always lower than those obtained from Batch tests, being between 1 and 2 orders of magnitude smaller for the simulations. Thus, as expected, the K_d parameter is lower in the field than from Batch tests, from which this parameter is usually obtained. The physical environment is much more heterogeneous and water generally circulates by preferential paths (De Gennes, 1983) (Jiménez-Martínez, et al., 2017). This fact reduces the specific surface in contact between the contaminant and the soil. This indicates the inappropriateness of Batch experiments in field-scale environmental studies.

Concerning the other Freundlich parameter, β, some discrepancies between measured and simulated results have been identified (Figure 7.C and .D). While very high concentrations were used and measured in the Batch tests, measured and simulated concentrations for all experiments were very small (> 0.2 ng/cm^3). Figure 12 shows isotherms using a generic K_d value (6 10^{-7} cm^3/ng) and $\beta > 1$ and $\beta < 1$ for concentrations used in Batch experiments. The maximum concentrations in dissolution (C_w) and adsorbed (C_s) measured in the flow cell experiments and simulated are depicted with a red shadow. This highlights the fact that small differences in β will not have a significant impact on the adsorbed mass of contaminant in our flow cell experiments and numerical simulations.

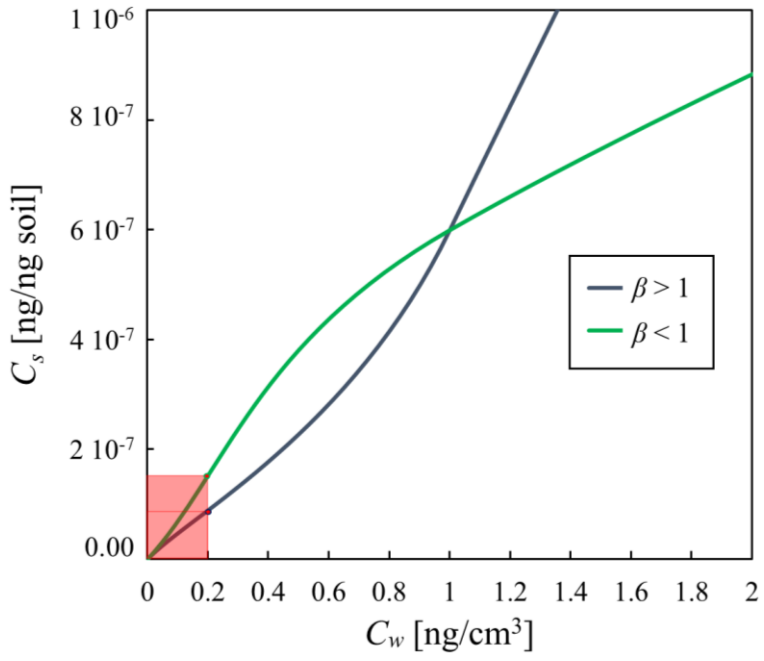

Figure 12. Freundlich isotherm plotted for $\beta > 1$ and $\beta < 1$ for a generic K_d value (6 10^{-7} cm^3/ng) value and experiments work area (red).

4. 3 Dependence on hydrocarbon chains and ethoxylated groups

Cationic surfactants with longer carbon chains adsorb more than those with shorter ones (Ersoy & Celik, 2003). Some studies concretize that for non-ionic surfactants, a reduction in hydrogen bonds explains the weaker effective attraction to the interfaces as concentration increases (Meconi, et al., 2016). Despite the low concentrations, no significant differences in K_d are recognized by carbon chains (Figure 7.A), neither measured or simulated. By ethoxylated groups, measured K_d for EO3 remained grouped and with a smaller average value, while EO6 and EO8 did not (Figure 7.B). The hydrogen bonding between EOs and functional groups on various soil components is probably the primary mechanism accounting for the preferential sorption of long EO homologs and is probably the reason for the lack of a strong correlation of sorption capacity with any soil component or property. Sorption of individual homologs within the mixture increased as EOs number increases (Yuan & Jafvert, 1997). Consequently, higher values were expected for groups EO6 and EO8 than for EO3. However, the similar values observed for the simulated K_d as a function of EOs can be explained by the low concentrations used and the possibility that underflow conditions these differences are hidden.

No significant differences were observed for β either measured or simulated by hydrocarbon chains (Figure 7.C). By ethoxylated groups, only the measured β differed for EO3, having a wider range of values, but not the simulated ones, which can be explained by the lower concentrations used in the flow cell experiments and simulations than in the Batch tests (Figure 7.D).

4. 4 Dependence on soil properties

From previous works, the adsorption dependence on clay and organic matter expected is as follows: (*i*) adsorption increases as clay content increases with the number of ethoxylated groups, and (*ii*) adsorption increases as organic matter content increases with the carbon chain length.

Figure 8 shows no differences in the K_d dependence on clay content by carbon chains and ethoxylated groups. Differences exist between measured and computed K_d values. Measured K_d values reached an asymptotic value for clay content > 2%, while computed ones remained more or less constant independently on the clay content. Similar behaviour is observed for K_d as a function of organic matter content (Figure 9). Note that both clay and organic matter content of the used soils is relatively low, which can explain the asymptotic (above certain clay content) and constant K_d values observed for measured and computed, respectively.

The exponent of the isotherm β did not present a clear trend with clay and organic matter content, having a high variability for measured ones and quasi constant value for simulated ones (Figures 10 and 11). While the variability in measured β is possible, the quasi constant value in the simulations is explained by the low concentrations used in the flow experiments (see also Figure 12).

Chapter 5

Conclusions

The methodology proposed, combining isotherms obtained from Batch experiments, flow cell (or column) experiments, and numerical simulations evidence the need of using with caution the isotherms obtained from batch experiments in studies to assess the environmental risk of non-ionic surfactants. The resulting K_d coefficients for non-ionic surfactants under flow/natural conditions, and obtained from numerical simulations, were always considerably smaller than those obtained from Batch tests, between 1 and 2 orders of magnitude, independently of the homolog (*i.e.*, carbon chain length and the number of ethoxylated groups). Batch test results also show that for the different carbon chain length studied, C16 shown a narrower range of K_d values, while the number of ethoxylated groups was more determinant than carbon chain length, having on average bigger K_d values as the number of ethoxylated groups increases. This was mainly due to the larger clay content than organic matter content (% of weight) in the soil samples used. However, a very similar range of K_d values was obtained from numerical simulations, independently of the carbon chain length and the number of ethoxylated groups. This is explained by the low concentration used in the experiments and simulations, and the fact that the adsorption process can be hidden by transport processes. The numerical results for the isotherm exponent, β, are less revealing and do not seem to depend on the variables considered in this study (*i.e.*, carbon chain length and the number of ethoxylated groups). Numerical results were very similar to the ones obtained from Batch experiments, with one exception: β for EO3, which shown a wider range in the measured case. Therefore, and due to commonly smaller concentrations found in the environment than the ones used in Batch tests, the uncertainty in the exponent β is less determinant than the one associated with the adsorption coefficient K_d for these contaminants.

No clear trends for measured K_d and β as a function of clay content and organic matter content were observed, independently of the homolog. Only highlight the asymptotic value reached by measured K_d for clay content > 2% and organic matter > 0.3%. Pretty stable simulated K_d and β values as a function of clay content and organic matter content were observed, independently of the homolog. The later evidences that for the low concentrations used in the flow cell experiments, and therefore in the simulations, transport processes can hide the impact of clay content and organic matter content on the adsorption processes.

Therefore, further studies with higher concentration of contaminants are recommended in order to better characterize the fate and transport of non-ionic surfactant homologs, in particular the impact of clay content and organic matter content, reducing the uncertainty in predictive models and the risk of contamination of groundwater bodies.

Bibliography

Bear, J., 1972. *Dynamics of Fluids in Porous Media.* New York: Dover Publications, Inc.

Brownawell, B. J., Chen, H., Zhang, W. & Westall, J. C., 1997. Sorption of Nonionic Surfactants on Sediment Materials. *Environmental Science & Technology.,* pp. 1735-1741.

Cano, M. & Dorn, P., 1996. Sorption of two model alcohol ethoxylate surfactants to sediments. *Chemosphere,* 33(6), pp. 981-94.

Carlsen, L., Mai-Britt Metzon & Jeanette Kjelsmark, 2002. Linear alkylbenzene sulfonates (LAS) in the terrestrial environment. *Science of the Total Environment,* pp. 225-230.

Connors, K. A., 1990. Chemical kinetics: the study of reaction rates in solution. s.l.:Wiley-VCH.

Corada-Fernández, C., Jiménez-Martínez, J., Candela. L, González-Mazo, E. & Lara-Martín, P. A., 2015. Occurrence and spatial distribution of emerging contaminants in the unsaturated zone. Case study: Guadalete River basin (Cadiz, Spain). *Chemosphere,* Volume 119, pp. S131-S137.

De Gennes, P., 1983. Hydrodynamic dispersion in unsaturated porous media. *Journal of Fluid Mechanics,* pp. 189-200.

Ding, J., Tsuzuki, T., McCormick, P. & Street, R., 1996. Ultrafine Cu particles prepared by mechanochemical process. *Journal of alloys and compounds,* 234(2), pp. L1-L3.

Droge, S. T. & Hermens, J. L., 2007. Nonlinear sorption of three alcohol ethoxylates to marine sediment: A combined Langmuir and Linear sorption process?. *Environmental Science & Technology,* 41(9), pp. 3192-3198.

Durán-Álvarez, J. C., Yamani Sánchez, Blanca Jiménez & Blanca Prado, 2014. The transport of three emerging pollutants through an agricultural soil irrigated with untreated wastewater. *Journal of Water Reuse and Desalination,* 4(1), pp. 1-9.

Eadsforth, C. et al., 2006. Monitoring of environmental fingerprints of alcohol ethoxylates in Europe and Canada. pp. 14-29.

Eichhorn, P., Silvana V. Rodrigues, Wolfram Baumann & Thomas PKnepper, 2002. Incomplete degradation of linear alkylbenzene sulfonate surfactants in Brazilian surface waters and pursuit of their polar metabolites in drinking waters. *Science of the Total Environment,* pp. 123-134.

El Rayis, O., 1985. Re-assessment of the titration method for determination of organic carbon in recent sediments. *Rapp. Comm. Int. Mer. Medit. 29,* pp. 45-47.

El-Kadi, A. & Ge, L., 1993. The Courant and Peclet number criteria for the numerical solution of the Richards equation. *Water Resources Research,* pp. 3485-3494.

Ersoy, B. & Celik, M. S., 2003. Effect of hydrocarbon chain length on adsorption of cationic surfactants. *Clays and Clay Minerals,* 51(2), pp. 172-180.

Gaudette, H., Flight, W., Torner, L. & Folger, 1974. An inexpensive titration method for the determination of organic carbon in recent sediments. *Journal of sedimentary research,* 44(1), pp. 249-253.

Gee, G. & Or , D., 2002. Methods of soil analysis. *Part 4, SSSA Book Series: 5.,* pp. 255-294.

González-Mazo, E., Lara-Martín, P. A. & Gómez-Parra, A., 2004. Determination and distribution of alkyl ethoxysulfates and linear Alkylbenzene sulfonates in coastal marine sediments from bay of Cadiz. *Environmental toxicology and chemistry,* 24(9), pp. 2196-202.

González-Mazo, E. et al., 2014. Occurrence, distribution and partitioning of nonionic surfactants and pharmaceuticals in the urbanized Long Island Sound Estuary (NY). *Marine Pollution Bulletin,* 85(2), pp. 710-719.

Grossman, R. B. & Reinsch, T., 2002. Bulk density and linear extensibility. *Methods of soil analysis,* Volume Part 4, SSSA Book Series: 5, Am. Soc. Agron., Madison, WI., pp. 201-228.

Guang-Guo, Y., 2006. Fate, behavior and effects of surfactants and their degradation products in the environment. *Environment International,* 32(3), pp. 417-431.

Henry, J. & Smith, J., 2002. The effect of surface-active solutes on water flow and contaminant transport in variably saturated porous media with capillary fringe effects. *Journal of Contaminant Hydrology,* 56(3-4), pp. 247-270.

Henry, J. & Smith, J., 2003. Surfactant-induced flow phenomena in the vadose zone: a review of data and numerical modeling. *Vadose Zone Journal,* pp. 154-67.

Hermens & Droge, 2009. Human and environmental risk assessment on ingredients of European household cleaning products. *HERA,* pp. 1-14.

Hildebrandt, A. et al., 2008. Impact of pesticides used in agriculture and vineyards to surface and groundwater quality (North Spain). *Water Research,* 42(13), pp. 3315-3326.

Jiménez-Martínez, J., Le Borgne, T., Tabuteau, H. & Méheust, Y., 2017. Impact of saturation on dispersion and mixing in porous media: photobleaching pulse injection experiments and shear-enhanced mixing model. *Water Resources Research,* 53(2), pp. 1457-1472.

John, D. M., House, W. A. & White, G. F., 2000. Environmental fate of nonylphenol ethoxylates: Differential adsorption of homologs to components of river sediment. *Environmental Toxicology and Chemistry,* pp. 293 - 300.

John, D. M., House, W. A. & White, G. F., 2009. Environmental fate of nonylphenol ethoxylates: Differential adsorption of homologs to components of river sediment. *Environmental Chemistry,* 19(2), pp. 293-300.

Kanokkarn, P., Takeo Shiina, Malee Santikunaporn & Sumaeth Chavadej, 2017. Equilibrium and dynamic surface tension in relation to diffusivity and foaming properties: Effects of surfactant type and structure. *Elsevier - Colloids and Surfaces A Physicochemical and Engineering Aspects,* pp. 135-142.

Kiewiet, A., de Beer KGM, Parsons JR & Govers HAJ, 1996. Sorption of linear alcohol ethoxylates on suspended sediment. *Chemosphere,* pp. 675-80.

Kolpin, W., Furlong, E.T., Meyer, M.T., Thurman, E.M & Zaugg, S.D., Barber, L.B, Buxton, H.T, 2002. Pharmaceuticals, hormones, and other organic wastewater contaminants in U.S. streams, 1999−2000: a national reconnaissance. *Environmental Science & Technology,* Volume 36, pp. 1202-1211.

Lara-Martín, P. A., E. González-Mazo & A. Gómez-Parra, 2006. Development of a method for the simultaneous analysis of anionic and non-ionic surfactants and their carboxylated metabolites in environmental samples by mixed-mode liquid chromatography–mass spectrometry. *Journal of Chromatography A,* pp. 188-197.

Lara-Martín, P. A., Gómez-Parra, A. & González-Mazo, E., 2008. Sources, transport and reactivity of anionic and non-anionic surfactants in several aquatic ecosystems from SW of Spain: a comparative study. *Environmental Pollution,* pp. 36-45.

Laurén, S., 2018. *Biolin Scientific.* [Online] Available at: https://blog.biolinscientific.com/author/susanna-lauren

Lee, J. F., Liao, P., Kuo, C.C & Yang, H.T.,Chiou, C.T., 2000. Influence of nonionic surfactant on contaminant distribution between water and several soil solids. *Journal of Colloid and Interface Science,* pp. 3022-28.

Lee, J., Hsu, M.H., Lee, C.K. & Chao, H.P., Chen, B.H, 2011. Effects of soil properties on surfactant adsorption. *Journal of the chinese Institute of engineers,* pp. 375-379.

Lord, D. L., Demond, A. H. & Hayes, K. F., 2000. Effects of organic base chemistry on interfacial tension, wettability, and capillary pressure in multiphase subsurface waste systems. *Transport in porous media,* pp. 38-79.

Lord, D. L., Demond, A. H., Salehzadeh, A. & Hayes, K. F., 1997. Influence of organic acid solution chemistry on subsurface transport properties. Capillary pressure-saturation. *Environmental Science & Technology,* pp. 2052-2058.

McAvoy, D. C. et al., 1998. Removal of alcohol ethoxylates, alkyl ethoxylate sulfates, and linear alkylbenzene sulfonates in wastewater treatment. *Environmental toxicology and chemistry,* pp. 1705-1711.

McAvoy, D., Ecknoff, W. & Rapaport, R., 1993. Fate of linear alkylbenzene sulfonate in the environment. *Environmental toxicology and chemistry,* pp. 977-987.

Meconi, G., Ballard, N., Asua, J. & Zangi, R., 2016. Adsorption and desorption behavior of ionic and nonionic surfactants on polymer surfaces. *Soft Matter,* 12(48), pp. 1-13.

Millington, R. J. & Quirk, J., 1961. Permeability of porous solids. *Transactions of the faraday society,* Volume 57, pp. 1200-1207.

Morrall, S., Eckhoff, W.S., Evans, A., Cano, M.L & Dunphy, J.C., McAvoy, D.C, 2006. Removal of alcohol ethoxylates and environmental exposure determination in the United States. *Ecotoxicology of environmental safety,* 64(1), pp. 3-13.

Mualem, Y., 1976. Hysteretical models for prediction of the hydraulic conductivity of unsaturated porous media. *Water Resources Research,* 12(6), pp. 1248-1254.

Neubecker, T., 1985. Determination of alkylethoxylated sulfates in wastewaters and surface waters. *Environmental Science & Technology,* 19(12), pp. 1232-6.

Oppel, J., Broll, G., Löffler, D & Meller, M., Röm, J, 2004. Leaching behaviour of pharmaceuticals in soil-testing-systems: a part of an environmental risk assessment for groundwater protection. *Science of the total environment,* 328(1-3), pp. 265-73.

Paweena, K., Santikunaporn, M., Shiina, T. & Chavadej, S., 2017. Equilibrium and dynamic surface tension in relation to diffusivity and foaming properties: effects of surfactant type and structure. *Colloids and surfaces a physicochemical and engineering aspects,* Volume 524, pp. 135-142.

Perfect, E., Sukop, M. C. & Haszler, G. R., 2002. Prediction of dispersivity for undisturbed soil columns from water. *Soil science society of america journal,* 66(3), pp. 696-701.

Podoll, R. T., Irwin, C. C. & Brendlinger, S., 1987. Sorption of water-soluble oligomers on sediments. *Environmental Science & Technology ,* 21(6), pp. 562-568.

Reynolds, W. & Elrick, D., 2002. Hydraulic Conductivity of Saturated Soils, Constant Head Method. In: Methods of Soil Analyses. *Physical Methods, Book Series 5, Soil Science Society of America, Madison, WI,* pp. 697-700.

Rodriguez, R. & Candela, L., 2005. Transport of Cr(VI), Ni(II) and Mn(II) through metallurgical wastes. Batch column experiments. *Dpt. of Geotechnical Engineering and Geosciences. School of Civil Engineering UPC,* pp. 64-77.

Salezadeh, A. & Demond, A. H., 1994. Apparatus for the rapid automated measurement of unsaturated soil transport properties. *Water Resources Research,* 30(10), pp. 2679-2690.

Schaap, M. G., Feike J. Leij & Martinus Th. van Genuchten, 2001. ROSETTA: a computer program for estimating soil hydraulic parameters with hierarchical pedotransfer functions. *Journal of Hydrology,* pp. 163-176.

Šimůnek, J., M. Th. van Genuchten & M. Šejna, 2006. The HYDRUS Software Package for Simulating Two- and Three Dimensional Movement of Water, Heat, and Multiple Solutes in Variably-Saturated Media. Version 1.0 ed. PC Progress, Prague, Czech Republic: 1-241.

Šimůnek, J., Van Genuchten, M. T. & Sejna, M., 2015. The HYDRUS-1D Software Package for Simulating the One-Dimensional Movement of Water, Heat, and Multiple Solutes in Variably-Saturated Media. *Department of Environmental Sciences, University of California Riverside, Riverside, CA, USA.*

Smith, J. & Gillham, R., 1994. The effect of concentration-dependent surface tension on the flow of water and transport of dissolved organic compounds: A pressure head-based formulation and numerical model. *Water Resources Research,* pp. 343-354.

Smith, J. & Gillham, R., 1999. Effects of solute concentration-dependent surface tension on unsaturated flow: laboratory sand column experiments. *Water Resources Research,* pp. 973-982.

Song, Q., Couzis, A., Somasundaran, P. & Maldarelli, P., 2006. A transport model for the adsorption of surfactant from micelle solutions onto a clean air/water interface in the limit of rapid aggregate disassembly relative to diffusion and supporting dynamic tension experiments. *Colloids and surfaces: physicochemical and engineering aspects,* Volume 282-283, pp. 162-182.

SRI Internacional, 1992. Surfactants, household detergents and their raw materials. *Chemical Economics Handbook.*

Szymanski, A., Wyrwas, B. & Lukaszewski, Z., 2003. Determination of non-ionic surfactants and their biotransformation by-products adsorbed on alive activated sludge. *Water Resource Research,* pp. 281-8.

Takada, H. & Ishiwatari, R., 1987. Linear alkylbenzene in urban riverine environments in Tokyo: distribution, sources and behavior. *Environmental Science & Technology,* p. 875–883.

Topp, E., Metcalfe, C., Edwards, M., Payne, M & Kleywegt, S., Russell, P., Lapen, Gottschall, N , 2012. Pharmaceutical and personal care products in groundwater, subsurface drainage, soil, and wheat grain, following a high single application of municipal biosolids to a field. *Chemosphere,* pp. 194-203.

Topp, E. et al., 2008. Runoff of pharmaceuticals and personal care products following application of biosolids to an agricultural field. *Science of the total environment,* pp. 52-59.

Travero-Soto, J. M., Brownawell, B. J., González-Mazo, E. & Lara-Martín, P. A., 2014. Partitioning of alcohol ethoxylates and polyethylene glycols in the marine environment: Field samplings vs laboratory experiments. *Science of the total environment,* pp. 671-678.

Tubau, I., Vázquez-Suñé, E., Carrera, J., González, S & Petrovic, M., López de Alda, M.J., Barceló, D, 2010. Occurrence and fate of alkylphenol polyethoxylate degradation products and linear alkylbenzene sulfonate surfactants in urban ground water: Barcelona case study. *Journal of Hydrology,* 383(1-2), pp. 102-110.

Van Compernolle, R., McAvoy, D.C., Sherren, A., Wind, T. & Cano, M.L., Belanger, S.E., Dorn, P.B., Kerr, K.M., 2006. Predicting the sorption of fatty alcohols and alcohol ethoxylates to effluents and receiving water solids. *Ecotoxicology and environmental safety,* 64(1), pp. 61-74.

van Genuchten, M., 1980. Closed-form equation for predicting the hydraulic conductivity of unsaturated soils. *Soil Science Society of America Journal.*

Vanderborght, J. & Vereecken, H., 2007. Review of dispersivities for transport modeling in soils. *Vadose zone journal,* pp. 1-24.

Wee, V., 1981. Determination of linear alcohol ethoxylates in waste and surface water. *Advances in the identification and analysis of organic pollutants in water,* p. 467.

Wind, T., Stephenson, R.J., Selby, M.A., Eadsforth., C.V & Sherren, A.J., Toy, R, 2006. Determination of the fate of alcohol ethoxylate homologs in a laboratory continuous activated-sludge unit study. *Ecotoxicology and environmental safety,* Volume 64, pp. 42-60.

Yekeen, N., Eswaran Padmanabhan, Ahmad Kamal Idris & Syed Muhammad Ibad, 2019. Surfactant adsorption behaviors onto shale from Malaysian formations: Influence of silicon dioxide nanoparticles, surfactant type, temperature, salinity and shale lithology. *Journal of Petroleum Science and Engineering,* pp. 841-854.

Yuan, C. & Jafvert, C. T., 1997. Sorption of linear alcohol ethoxylate surfactant homologs to soils. *Journal of contaminant hydrology,* 28(4), pp. 311-325.

Yun-Hwei, S., 2000. Sorption of non-ionic surfactants to soil: the role of soil mineral composition. *Chemosphere,* pp. 711-716.

Appendix

A. Surfactants total concentrations profiles: soil core 1

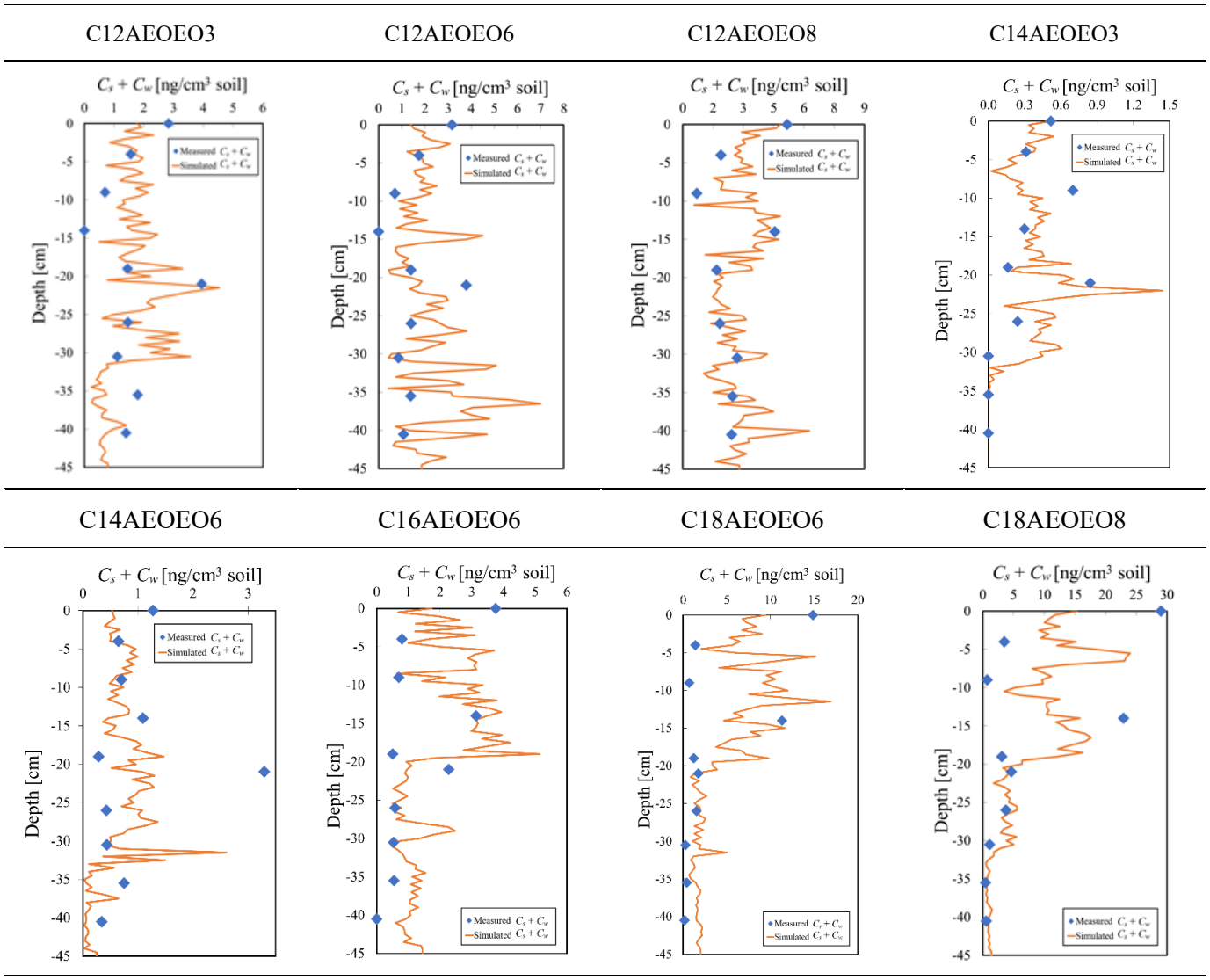

Figure 13. Soil core 1 measured (rhomboids) and simulated (solid line) total concentration (Cs + Cw) [ng/cm3 of soil] for different surfactants (C1XAEOEOX) at different depths.

B. Surfactants total concentrations profiles: soil core

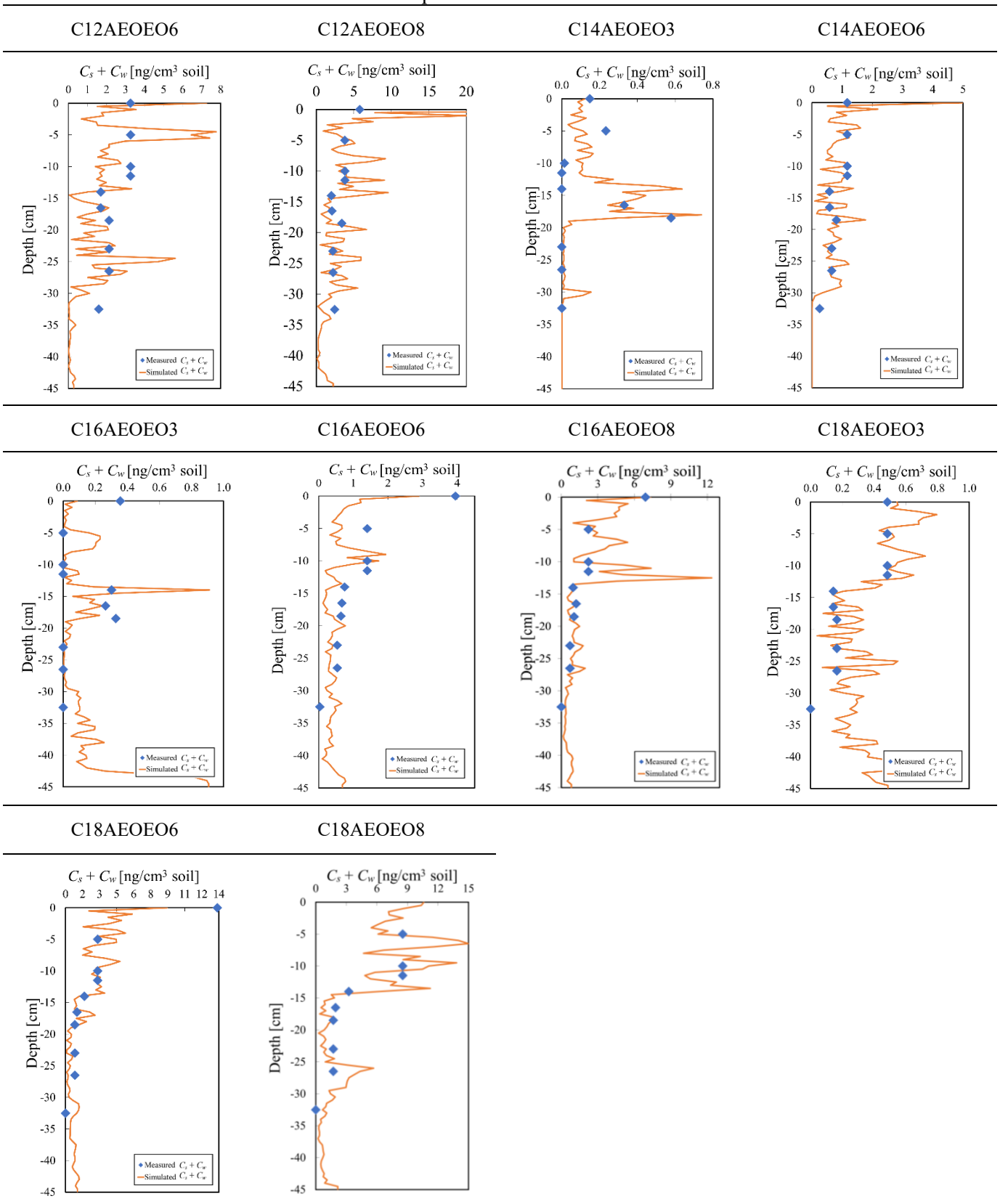

Figure 14. Soil core 2 measured (rhomboids) and simulated (solid line) total concentration (Cs + Cw) [ng/cm3 of soil] for different surfactants (C1XAEOEOX) at different depths.

C. Negligible effect on non-ionic surfactants at low concentrations (Paweena, et al., 2017).

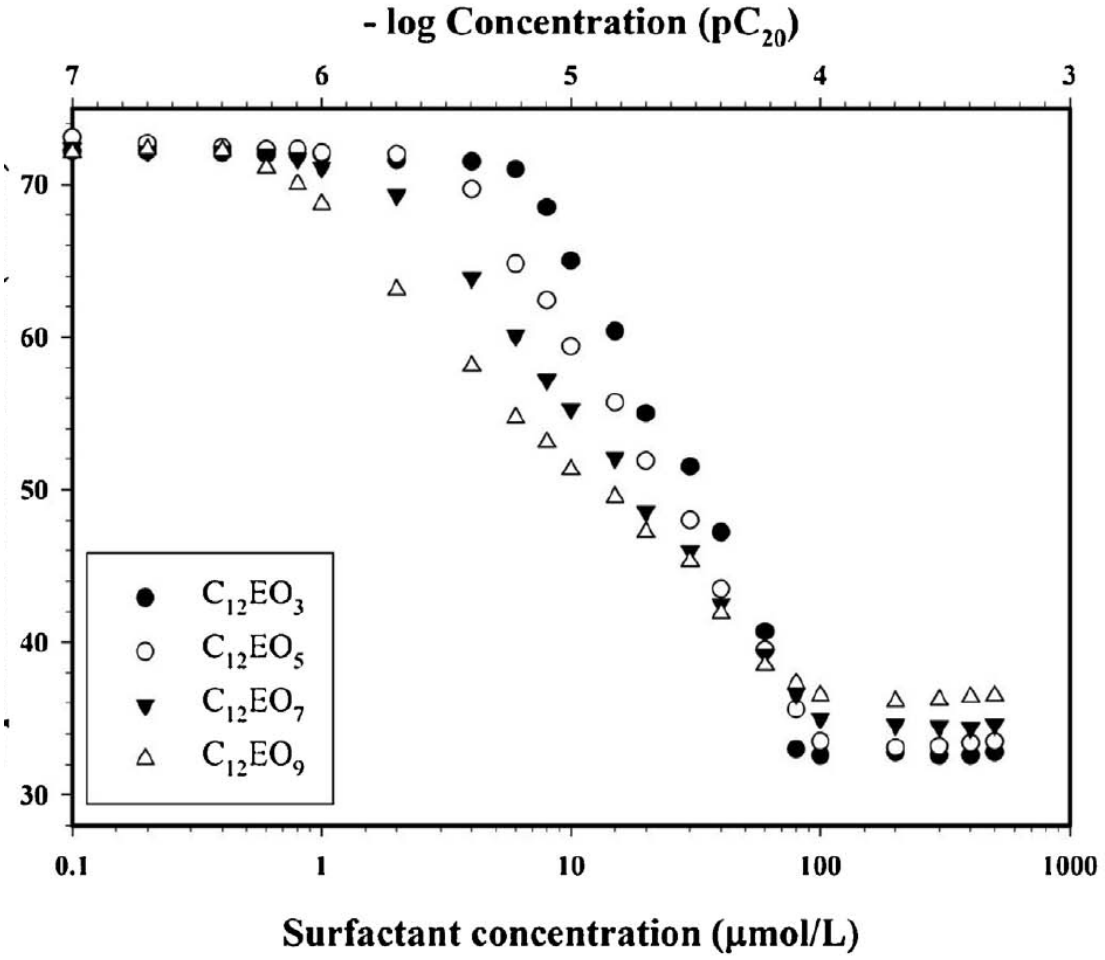

Figure 15. Surface tension of surfactant solution as a function of concentration C12EOn with different amounts of EO units.